Efficient linearization of the augmented plane-wave method

Georg K. H. Madsen,[1] Peter Blaha,[1] Karlheinz Schwarz,[1] Elisabeth Sjöstedt,[2] and Lars Nordström[2]
[1] *Technische Universität Wien, Getreidemarkt 9/156, A-1060 Vienna, Austria*
[2] *Condensed Matter Theory Group, Physics Department, Uppsala University, S-75121 Uppsala, Sweden*
(Received 14 January 2001; revised manuscript received 21 March 2001; published 30 October 2001)

We present a detailed analysis of the APW+lo basis set for band-structure calculations. This basis set consists of energy independent augmented plane-wave (APW) functions. The linearization is introduced through local orbitals evaluated at the same linearization energy as the APW functions. It is shown that results obtained with the APW+lo basis set converge much faster and often more systematically towards the final value. The APW+lo thereby allows accurate treatment of systems that were previously unaccessible to linearized APW. Furthermore, it is shown that APW+lo converges to the same total energy as LAPW provided the higher angular momenta l are linearized, either by adding extra local orbitals or treating them by LAPW. It is illustrated that the APW basis functions are much closer to the true form of the eigenfunctions than the LAPW basis functions. This is especially true for basis functions that have a strong energy dependence inside the sphere.

DOI: 10.1103/PhysRevB.64.195134 PACS number(s): 71.15.Ap, 71.20.−b, 71.15.Nc, 31.15.Ew

I. INTRODUCTION

A natural basis for calculating the k-dependent one-electron wave functions in periodic solids are plane waves (PW's). They are, however, a very inefficient basis set for describing the rapidly varying wave function close to the nuclei. In order to overcome this difficulty one can either eliminate these oscillations, due to the presence of the core electrons, as done in pseudo potential calculations or one can use a mixed basis set. One example of the latter approach was introduced by Slater who suggested the augmented plane waves (APW's) (Refs. 1 and 2) as basis functions for solving the one electron equations, which now correspond to the Kohn-Sham equations within density functional theory. In the APW scheme the unit cell is divided into two regions: (i), The muffin-tin (MT) region which consists of spheres centered at the atomic position, inside which the APW's satisfy the atomic Schrödinger equation, and (ii) the interstitial region I, where the APW's consist of PW's,

$$\phi_{\mathbf{K}}(\mathbf{r})=\begin{cases}\sum_L a_L^{\alpha\mathbf{K}} u_l^{\alpha}(r',\epsilon)Y_L(\hat{\mathbf{r}}') & r'<R_{MT}^{\alpha}\\ \Omega^{-1/2}\exp[i(\mathbf{k}+\mathbf{K})\cdot\mathbf{r}] & r\in I\end{cases}. \quad (1)$$

Ω is the unit-cell volume, $\mathbf{r}'=\mathbf{r}-\mathbf{r}_\alpha$ where $\mathbf{r}_\alpha$ is the atomic position within the unit cell, R_{MT}^{α} is the radius of the MT sphere, L is the reduced angular momentum index $\{lm\}$, $\mathbf{k}$ is a wave vector in the irreducible Brillouin zone (IBZ) and $\mathbf{K}$ is a reciprocal-lattice vector. u_l^{α} is the numerical solution to the radial Schrödinger equation at the energy ϵ. The coefficients $a_L^{\alpha\mathbf{K}}$ are chosen such that the atomic functions, for all L components, match the PW with $\mathbf{k}+\mathbf{K}$ at the MT sphere boundary. Inside the MT sphere a Kohn-Sham orbital $\psi_i(\mathbf{r})$ can only be accurately described if ϵ is equal to the eigenenergy ε_i of $\psi_i(\mathbf{r})$. Therefore a different energy dependent set of APW basis functions must be found for each eigenenergy. This is the main drawback of the APW method, since the energy dependent basis set leads to a nonlinear eigenvalue problem which computationally is very demanding.

Linearizing APW

1. LAPW

There were several attempts to improve the energy dependance of the secular equations but the first really successful one was the linearization by Andersen.[3] This work led to the first implementation of the linearized augmented plane-wave (LAPW) method.[4] In the LAPW method the energy dependence of the radial functions inside each sphere is linearized by adding a second term to the radial part of the basis functions,

$$\phi_{\mathbf{K}}(\mathbf{r})=\begin{cases}\sum_L [a_L^{\alpha\mathbf{K}} u_{1l}^{\alpha}(r')+b_L^{\alpha\mathbf{K}}\dot{u}_{1l}^{\alpha}(r')]Y_L(\hat{\mathbf{r}}') & r'<R_{MT}^{\alpha}\\ \Omega^{-1/2}\exp[i(\mathbf{k}+\mathbf{K})\cdot\mathbf{r}] & r\in I\end{cases}. \quad (2)$$

u_{1l} is the solution to the radial Schrödinger equation at a fixed linearization energy ϵ_{1l} and $\dot{u}_{1l}$ is its energy derivative computed at the same energy. The LAPW's provide a sufficiently flexible basis to properly describe eigenfunctions with eigen-energies around the linearization energy. This has the important consequence that the ϵ_{1l} values can be kept fixed and all eigenenergies can be obtained with a single diagonalization.

LAPW's, however, are not suited for treating states that lie far from the linearization energy, such as so-called semicore states that have a principal quantum number one less than the corresponding valence state. Furthermore, the linearization is not sufficiently accurate for broad valence bands if the partial wave shows a large energy variation inside the MT sphere (such as d or f states). To improve the linearization Singh introduced local orbitals (LO's) to augment the LAPW basis set for certain l values,[5]

$$\phi_{LO}(\mathbf{r})=\begin{cases}[a_L^{\alpha,LO}u_{1l}^{\alpha}(r')+b_L^{\alpha,LO}\dot{u}_{1l}^{\alpha}(r')+c_L^{\alpha,LO}u_{2l}^{\alpha}(r')]Y_L(\hat{\mathbf{r}}') & r'<R_{MT}^{\alpha}\\ 0 & r\in I\end{cases}. \tag{3}$$

An LO is constructed by the LAPW radial functions at the energy ϵ_{1l} and a third radial function $u_{2l}(r')$ at a second energy ϵ_{2l}, chosen to most efficiently improve the linearization. The three coefficients are determined by the requirements that the LO's should have zero value and slope at the MT sphere boundary and the normalization. LO's were found to be more efficient in improving the linearization than alternative methods with APW's having continuous second and third derivatives.[5]

2. APW+lo

Recently Sjöstedt *et al.* suggested an important modification of the LAPW method.[6] They introduced an APW+lo basis, where the APW's, Eq. (1), are evaluated at a fixed energy and flexibility is added by including another type of local orbitals (denoted as lo's) combining a u and $\dot{u}$,

$$\phi_{lo}(\mathbf{r})=\begin{cases}[a_L^{\alpha,lo}u_{1l}^{\alpha}(r')+b_L^{\alpha,lo}\dot{u}_{1l}^{\alpha}(r')]Y_L(\hat{\mathbf{r}}') & r'<R_{MT}^{\alpha}\\ 0 & r\in I\end{cases}. \tag{4}$$

The lo's are evaluated at the same fixed energy as the corresponding APW's. The two coefficients are determined by the normalization and the condition that $\phi_{lo}(R_{MT})$ has zero value. In this version the $\dot{u}_l$ is independent from the PW's and only included for a chosen set of ''physically important'' l-quantum numbers.

Already Koelling and Arbman pointed out that LAPW converges somewhat slower than the APW method with respect to the number of basis functions.[4] The LAPW basis functions are required to be differentiable at the MT boundary and are therefore not optimally suited for describing the orbitals inside the sphere. Such constraints are not introduced on the APW basis set when the energy derivatives are included in form of local orbitals.[6]

In the APW+lo method the energy derivative term is only included in a few lo's and not in every PW, as in LAPW. It is therefore not obvious that the linearization of the APW+lo basis is as accurate as the LAPW scheme in all cases. We therefore aim to demonstrate that APW+lo not only converges faster towards the basis set limit, but can also reach the same accuracy as LAPW. We have implemented the APW+lo method into the WIEN97 code.[7] This has been done in a flexible manner so that LAPW and APW+lo basis functions can be mixed, meaning that some l-quantum numbers in the expansion inside a sphere can include energy derivatives, Eq. (2), while others may be treated as APWs, Eq. (1), at fixed energy with added lo's, Eq. (4). We test different systems and explore the possibility of mixing LAPW and APW+lo basis sets. The main objective of this paper is to compare the APW+lo basis set with the LAPW basis set, but not with experimental results as such comparisons will be influenced by inadequacies in the applied density functional. Neither the APW's, the lo's, nor the LO's are required to be continuous in slope at the MT-sphere boundary. This complication makes it necessary to include surface terms in the calculation of the Hamiltonian and the forces, as described in detail in the appendixes.

II. RESULTS AND DISCUSSION

In the following we will present a study of the convergence of the total energy and the electric-field gradient (EFG) in Cu_2O. By varying the unit-cell volumes of GaAs and body-centered cubic (bcc) Fe we explore the influence of the basis set on the total energy further. The resulting total energies are fitted to the Birch-Murnaghan equation from which the equilibrium unit-cell volumes and bulk moduli are derived. Optimization of structures with atoms placed at free fractional coordinates is greatly simplified by using forces[8] instead of numerically calculated energy derivatives. The implementation of analytically calculated forces within the APW+lo method is described in the appendixes. In the final subsection we apply this to sodium electrosodalite.

Several combinations of augmentations within the spheres will be tested and are summarized in Table I together with a ''label'' to introduce a shorthand notation used later on. Results will be reported in terms of Rk_{max} (calculated as the largest PW $|K+k|$ times the smallest MT sphere radius), which is a reasonably transferable indicator of basis set quality, and in terms of the number of PW's used in the calculation which determines the actual computational effort. In all calculations the linearization energies of the APW's and lo's and the LAPW's were set in the valence region. The energies of the semicore LO were set to the mean of the energies E_{top} (where u_l changes sign in value) and E_{bottom} (where u_l

TABLE I. Different basis sets employed in the present calculations. The number of LO's depends on the system studied (see Table II).

Label	Basis set inside spheres
LAPW	LAPW's for all l
APW+lo	APW's for all l + lo's for all physically important l
APW+lop	APW's for all l + lo's for all physically important l and the first polarization l.
L/APW+lo	APW's for all l + lo's for all physically important l LAPW's for all polarization l
LAPW/dAPW	LAPW's for all l except $l=2$ for which APW+lo is used

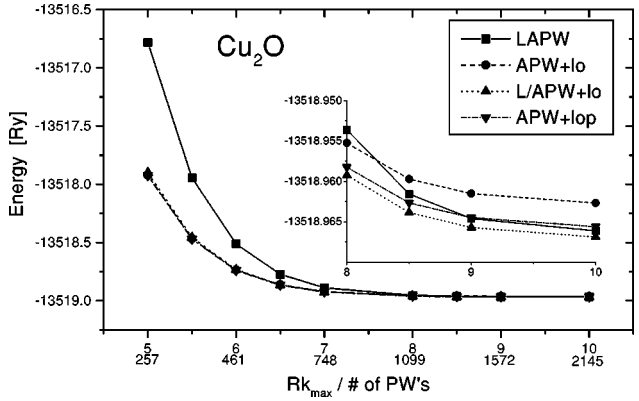

FIG. 1. Total electronic energy per formula unit in Cu_2O. The curves are marked as explained in Table I. The number of PW's is for $\mathbf{k}=2\pi/a(1/12,1/12,1/12)$.

changes sign in slope), as is standard in the WIEN97 code.[7] The energies were always set to the same in the compared APW+lo and LAPW calculations.

A. Cu_2O

Cuprite, Cu_2O, forms a highly symmetric (simple cubic) relatively open crystal structure. The oxygen atoms form a bcc sublattice and each oxygen atom is tetrahedrally coordinated to four copper atoms each of which is twofold coordinated to two oxygen atoms. All calculations in this section have been carried out with LOs added for the Cu $3p$, $3d$, and the O $2s$ states. The IBZ was sampled on a tetrahedral mesh with six intervals in each direction.[9] The muffin-tin sphere radius was set to 1.85 a.u. and 1.6 a.u. for Cu and O, respectively.

Figure 1 shows the total energy of Cu_2O as a function of Rk_{max} for four different types of basis sets. The curve marked LAPW corresponds to a pure LAPW basis set and the curve marked APW+lo corresponds to a pure APW basis set with lo's added for $l\leqslant 2$ on Cu and $l\leqslant 1$ on O. The APW+lo method thus contains 44 additional lo's compared to the LAPW basis set, Table II. Both basis sets contain the LO's mentioned above. In agreement with the original study[6] it can be seen that APW+lo converges much faster than LAPW. The APW+lo total energy is converged to within 10 mRy of the final value at $Rk_{max}=8$ corresponding to approximately 1100 PW's while the LAPW basis set needs a cutoff defined by $Rk_{max}=8.5$, corresponding to approximately 1330 PW's, to reach the same precision.

However, it should also be pointed out that at very high PW cutoffs the LAPW basis set gives a lower energy than the APW+lo, see inset in Fig. 1. Although the energy difference is small, this is worth investigating. There seems to be three possible reasons for this deviation: (i) there are remaining kinks in the APW eigenfunctions which will raise the kinetic energy, see Eq. (A1) in Appendix A, (ii) the $b_L^{\alpha,lo}\dot{u}_{1l}^{\alpha}(r')$ term is only included in a few lo's which could mean that the linearization of the APW+lo basis set is less accurate than the LAPW scheme, or (iii) in the APW+lo method only the l-quantum numbers with added lo's are linearized in energy and the behavior in Fig. 1 could mean that the orbitals of higher angular momenta than the "physically important" need to be linearized as well.

TABLE II. Number of basis functions used in calculation. The quoted number of PW corresponds to what has been judged as a converged calculation. See text for details.

		LAPW	APW+lo L/APW+lo	APW+lop
Cu_2O	LO	18	18	18
	lo		44	82
	PW	750	350	350
GaAs	LO	11	11	
	lo		18	
	PW	330	160	
SES	LO	92	92	
	lo		176	
	PW	6490	2941	
		LAPW	APW+lo	LAPW/dAPW
Fe	LO	8	8	8
	lo		9	5
	PW	52	43	43

If (iii) is valid, a basis set containing lo's for polarization quantum numbers (in this context we call higher l values that are not present in the atomic calculation polarization quantum numbers) should converge to the same total energy as LAPW. The curve marked APW+lop, which corresponds to an APW basis set with lo's added up to the first set of polarization quantum numbers (for Cu $l\leqslant 3$ and for O $l\leqslant 2$), shows that this is indeed the case. Though the inclusion of lo's for the first polarization quantum number adds 38 basis functions, the APW+lop basis still needs significant fewer basis functions than the LAPW basis set.

A different solution to (iii) could be a hybrid basis set, namely to treat the physically important orbitals as APW with added lo's but the polarization l-quantum numbers with LAPW. Such a basis set, marked L/APW+lo in Fig. 1, converges to the same total energy as the LAPW basis set. It can also be seen that the mixed L/APW+lo basis set converges as fast as the APW+lo basis set which means that LAPW are as efficient as APW basis functions for describing polarization orbitals. The APW radial functions are optimally suited for describing the atomiclike behavior of the wave function close to the atomic positions.[6] However, the polarization functions on an atom are mainly needed to describe the tails of the wave functions from surrounding atoms reaching into its MT sphere and therefore are not better described by APW's than LAPW's. The importance of polarization orbitals will thus depend on the local symmetry. This explains why in the original work,[6] where only results for two closed packed fcc systems were presented, APW+lo was found to converge to the same total energy as LAPW despite lo's only being added for physically important l-quantum numbers.[6]

The EFG tensor is sensitive to the anisotropy of the charge distribution close to the nucleus and can be calculated

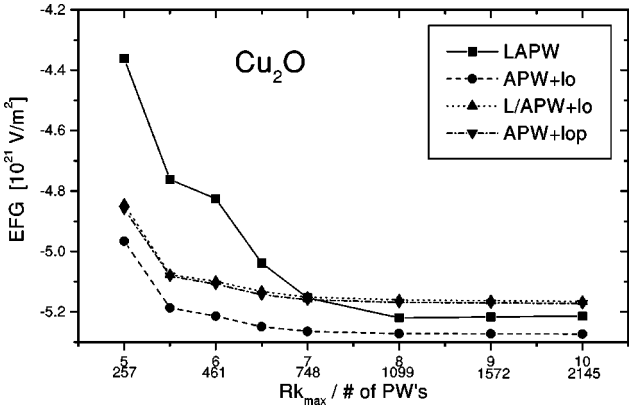

FIG. 2. Calculated EFG at the Cu site in Cu_2O at experimental unit-cell volume. The number of PW's is for $\mathbf{k}=2\pi/a(1/12,1/12,1/12)$.

from first principles.[10] The EFG serves as a critical test for the quality of the wave function or corresponding density. In Cu_2O the copper atoms are located on the threefold axes which means that the EFG tensor is diagonal and described by its principal component. In Fig. 2 the calculated EFG at the Cu site is plotted as a function of basis set convergence. When employing an LAPW basis set the EFG at the copper site is converged to within 2% of the final value at a PW cutoff defined by $Rk_{max}=7$ corresponding to about 750 PW's. With an APW+lo basis set a similar precision is reached at a PW cutoff defined by $Rk_{max}=5.5$, i.e., about 350 PW's, which is a very significant reduction in basis set size. It should be pointed out that the present calculated EFG value differs significantly from the earlier LAPW study where a value of 8.26×10^{21} V/m^2 was reported.[11] The old calculation was performed without LO's and the Cu $3p$ state was treated in an energy window separate from the valence states. In this approximation the $3p$ states were not strictly orthogonal to the valence states.

B. GaAs

The discussion above showed that the two basis sets APW+lop and L/APW+lo behave similarly and consequently we just present results for the latter in the following two examples. GaAs is a semiconductor and forms a noncentrosymmetric diamond lattice. The calculations on GaAs were carried out with LO's added for the Ga $3d$ and As $3d$ and $3s$ states. The IBZ was sampled on a tetrahedral mesh with ten intervals in each direction. The MT sphere radii for both Ga and As were set to 2.0 a.u.

Figure 3(a) shows that the equilibrium volume converges much faster with APW+lo than with LAPW. Interestingly, the fastest convergence is with the L/APW+lo basis set which means that the equilibrium volume is converged already at a PW cutoff defined by $Rk_{max}=6.5$, corresponding to approximately 160 PW's, whereas LAPW requires $Rk_{max}=8$, i.e. about 330 PW's, to reach similar precision. Furthermore the APW+lo and the L/APW+lo give equilibrium volumes within 3% of the final result even at a poorer cutoff defined $Rk_{max}=6$. The calculated bulk modulus of

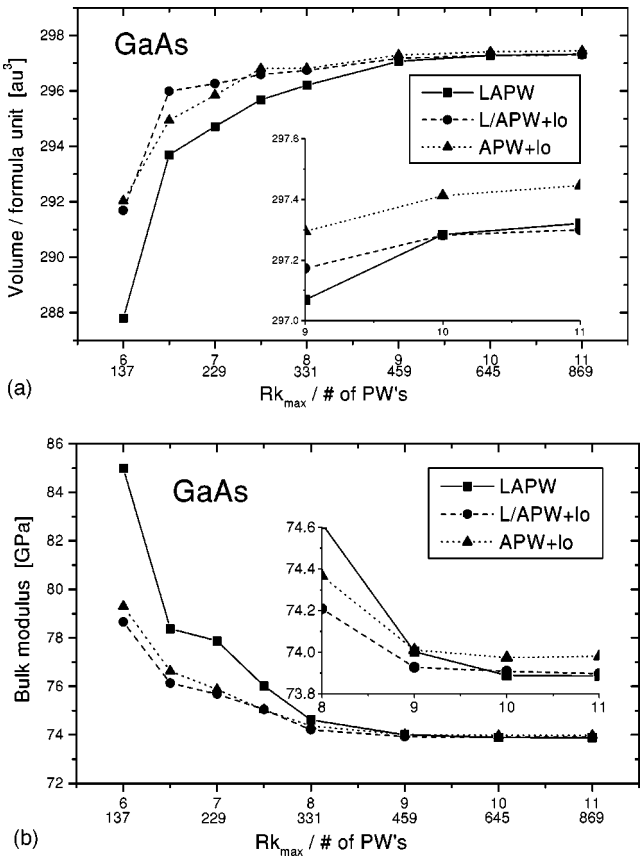

FIG. 3. (a) Calculated equilibrium lattice constants and (b) bulk moduli of GaAs. The number of PW's is for the Γ point and the experimental volume.

GaAs, Fig. 3(b), shows a similar behavior as the equilibrium volume. With the L/APW+lo basis it is converged to within 3% of the final value with $Rk_{max}=6.5$ (160 PW's) whereas LAPW requires $Rk_{max}=7.5$ (285 PW's), to reach similar precision. The insets in Figs. 3(a) and 3(b) show that the hybrid L/APW+lo converges to exactly the same values as LAPW whereas the pure APW+lo values slightly deviates.

C. bcc Fe

The calculations on bcc Fe were carried out with a MT radius of 2.0 a.u. and with LO's added for the $3d$ and $3p$ states. The IBZ was sampled on a tetrahedral mesh with 19 intervals in each direction.

Figure 4 shows a behavior similar to GaAs: The APW+lo and L/APW+lo methods converge faster than the pure LAPW basis set and only L/APW+lo converges to the same unit-cell volume as the LAPW basis set. The actual number of basis functions saved when going from LAPW to APW is very small as could be expected for this relatively densely packed structure. The calculated bulk modulus does not converge smoothly, Fig. 4(b). This is because the actual number of PW's in a series of calculations can vary strongly with unit-cell volume at low PW cutoff. For example a unit cell volume of 68 a.u.^{3} at $Rk_{max}=6$ gives 19 PW's , while a unit-cell volume of 84 a.u.^{3} gives 40 PW's. The bulk modulus calculated at $Rk_{max}=6$ with APW+lo and L/APW+lo

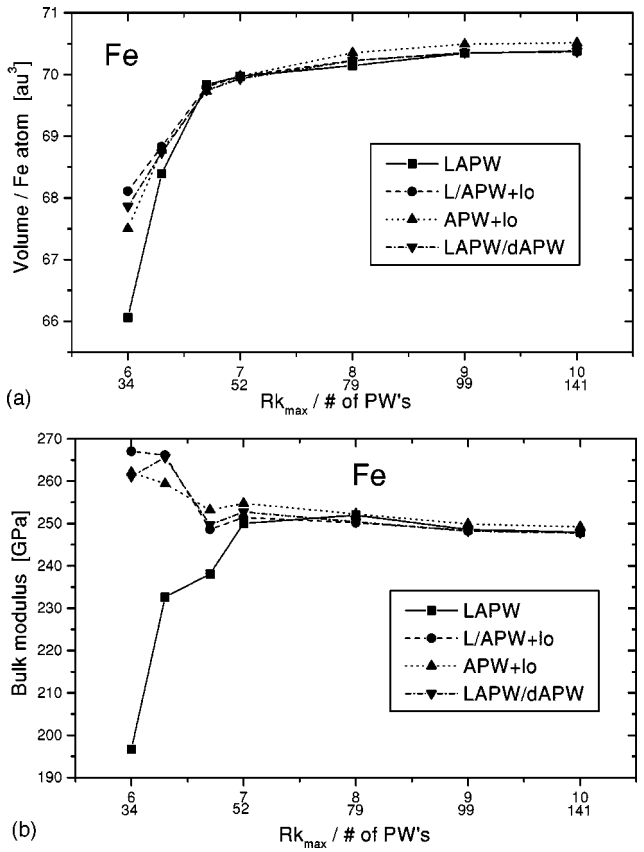

FIG. 4. (a) Calculated equilibrium lattice constants and (b) bulk moduli of bcc Fe. The number of PW's is for the $\mathbf{k}=2\pi/a(1/19,1/19,1/19)$ and experimental volume.

agree much better with the final value than LAPW. This indicates that APW is less sensitive to the number of PW's in the basis set. It is well known that systems such as Fe with *d*-orbitals close to the Fermi level need high PW cutoffs in LAPW. To illustrate this we have constructed a basis set which treats all *l*-quantum numbers as LAPW's except $l=2$ which is treated as APW+lo. As seen in Fig. 4 the LAPW/*d*APW performs just as well as the APW+lo and L/APW+lo basis sets.

The above LAPW/*d*APW basis set underlines that the *s* and *p* orbitals converge much faster in LAPW than the *d* orbitals and that the main improvement in the APW basis set is a better description of the *d* part of the basis functions. A PW cutoff defined by $Rk_{max}=5.5$ at primitive unit-cell volume 75.7 a.u.^{3} corresponds to 19 PW's. The basis set then consists of only the (000) PW, the 12 PW's in the (110) star, and 6 PW's in the (200) star. At the Γ point the (000) PW and the (200) star of PW's do not contribute to the *d* orbitals of t_{2g} symmetry, which thus are described by only one star of PW's. When no *d*-LOs are added this correponds to a minimal PW basis set and the calculated valence electron density will therefore be extremely sensitive to the shape of the basis functions. Figure 5(a) shows how close to the converged density the minimum APW basis set gets while the LAPW basis set is clearly far off. The improved description of the *d*-part of the basis functions is explained in Fig. 5(b). The radial components u and $\dot{u}$ of the *d* partial wave in Fe are

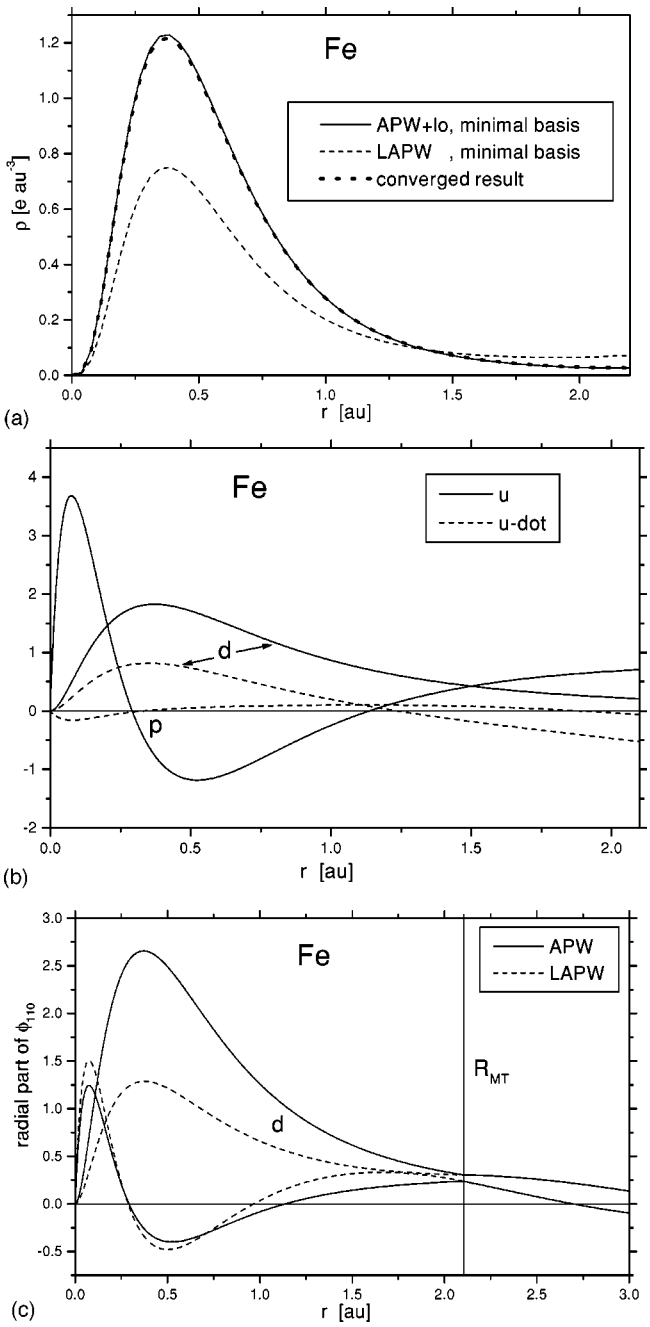

FIG. 5. (a) The spin-up valence electron density of the t_{2g} orbitals along the [111] direction calculated at the Γ point. The density for APW+lo and LAPW are both calculated with the minimal basis set (described in text) using the potential from the converged density. (b) shows the radial part of the *p* and *d* functions in Fe (full lines: APW; dashed lines: LAPW) matched to the 110 star PW's in the interstitial. (c) $u(r')$ and $\dot{u}(r')$ for the Fe *p* and *d* orbitals evaluated at the energies $\epsilon_p=0.400$ Ry and $\epsilon_d=0.468$ Ry.

shown. It can be seen that the strong energy dependence of the *d* radial function leads to a relative large $\dot{u}$, while the $\dot{u}$ of the *p* radial function is only a small correction. Figure 5(c) shows the radial part of the *d* and *p* parts of a $\phi_{(110)}$ APW/LAPW basis functions. The APW's have kinks at R_{MT}, while the LAPW's have continuous first derivatives. The

large $\dot{u}$ of the d radial function leads to a considerable deformation of the d-LAPW basis function. The p-LAPW is much less affected, despite the discontinuity in the first derivative being larger than in the d part.

D. Sodium electro sodalite

As a further test case we have calculated the forces in sodium electro sodalite (SES) at the structure published by Madsen *et al.*[12] SES is an interesting structure in which the alumina-silicate sodalite framework supports a paramagnetic Na_4^{3+} cluster inside each cage. It has been chosen as a test case because the structure contains large interstitial holes. Furthermore, due to the short Si–O and Al–O bond distances, rather small Si (1.55 a.u.), Al (1.70 a.u.), and O (1.5 a.u.) sphere radii must be used. The sodium is weakly bound to the framework and thus a MT sphere with $R_{MT}=2.0$ a.u. was used. Semicore LO were added to improve the description of the silicon and aluminum $2p$, the oxygen $2s$ orbitals, and the sodium $2s$ and $2p$ states. The IBZ was sampled on a tetrahedral mesh with three intervals in each direction. Again, as the main purpose of this work is to compare computational methods, the calculations have been done in a hypothetical nonmagnetic phase and not in the experimental antiferromagnetic ground state.

The space group is $P\bar{4}3n$ and the oxygens are placed on general crystallographic positions with three free positional parameters. The sodiums are found on the threefold screw axis and its position is described by only one parameter. Figure 6 shows the calculated forces on the oxygen and sodium atoms as a function of PW cutoff. As was also seen for the O_2 molecule,[13] the forces calculated with APW+lo converge much faster than the force calculated with LAPW. The APW forces converge to within 4 mRy/a.u. at $Rk_{max}=5$ (2941 PW's) while an LAPW basis set need a PW cutoff of $Rk_{max}=6.5$ (6490 PW's). It is also important to note that the forces calculated with the APW+lo method converge much smoother towards the final values. This means that even at a PW cutoff corresponding to $Rk_{max}=4.5$ (2124 PW's) the forces point in the right direction whereas the smallest usable LAPW basis set needs a PW cutoff of $Rk_{max}=6$ (5088 PW's). This means that the first steps of a structure relaxation in APW+lo can be carried out with a rather small basis set.

Figure 6(b) shows the force on the sodium atom. As the sodium MT sphere is bigger than the oxygen sphere the force is more converged at a lower PW cutoff. However, the advantage of APW+lo is still evident as the force is completely converged already at a cut-off defined by $Rk_{max}=4$ while LAPW needs a cutoff of $Rk_{max}=6.5$ to reach a similar accuracy.

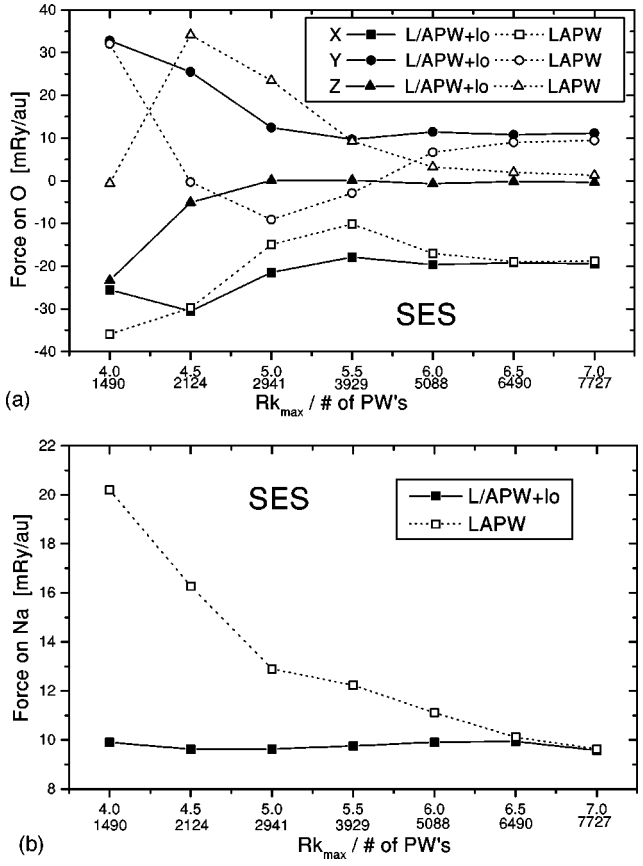

FIG. 6. Atomic forces on (a) oxygen and (b) Na in the NM SES. The number of PW's is for the $\mathbf{k}=2\pi/a(1/6,1/6,1/6)$ point.

III. COMPUTATIONAL CONSIDERATIONS

The scaling of the computationally dominant parts is given in Table III. Both the number of valence bands and the number of basis functions needed scale linearly with the number of atoms. The overall scaling of LAPW and APW+lo is therefore N_{at}^3. The improved efficiency APW+lo has two origins: (i) fewer basis functions are needed per atom and (ii), the form of the APW basis functions is simpler since the $b_L^{\alpha}\dot{u}_{1l}^{\alpha}(r')$ term appears only in a few lo's.

The lower number of basis functions per atom needed for the same accuracy has been documented in the previous sections. For covalently bonded open systems savings about 50% in the number of basis functions has been achieved. This means a speed up by a factor 4 in the setup of the secular matrices and the iterative diagonalization[14] and by a factor 8 for a full diagonalization which are the computationally dominant parts of the SCF cycle, Table III.

The simpler form of the basis functions does not affect the diagonalization but can significantly decrease the amount of time needed for the setup of the matrices. This is especially evident in the setup of the nonspherical part of the full po-

TABLE III. Scaling per k point. N_{at} is the number of atoms. N_b is the number of valence bands, n_L is the number of $\{lm\}$ pairs in Eq. (1) or Eq. (2). M is the number of basis functions.

Task	Scaling
Matrix setup	$n_L^2 N_{at} M^2$
Full diagonalization	M^3
Iterative diag.	$N_b M^2$
Calculation of ρ	$n_L N_b N_{at} M$

tential Hamilton matrix,[15] which involves calculating the sums

$$H^{NS,\alpha}_{\mathbf{K},\mathbf{K}'} = \sum_{L'} \Bigg(a^{\alpha,\mathbf{K}'}_{L'} \sum_{L} \left[a^{\alpha,\mathbf{K}*}_{L} \langle u^{\alpha}_{l} | V_{NS} | u^{\alpha}_{l'} \rangle + b^{\alpha,\mathbf{K}*}_{L} \langle \dot{u}^{\alpha}_{l} | V_{NS} | u^{\alpha}_{l'} \rangle \right] + b^{\alpha,\mathbf{K}'}_{L'} \sum_{L} \left[a^{\alpha,\mathbf{K}*}_{L} \langle u^{\alpha}_{l} | V_{NS} | \dot{u}^{\alpha}_{l'} \rangle + b^{\alpha,\mathbf{K}*}_{L} \langle \dot{u}^{\alpha}_{l} | V_{NS} | \dot{u}^{\alpha}_{l'} \rangle \right] \Bigg) \langle Y^{*}_{L} | Y_{L'} \rangle K_{\alpha}, \tag{5}$$

where V_{NS} is the nonspherical part of the potential and K_α are the lattice harmonics combatible with the local site symmetry.

With an APW basis set this reduces to a double sum over only one term, thereby reducing the time for setup of the Hamilton matrix by a factor 4. For cases such as the sodalite and Cu_2O, where only half the number of basis functions are needed compared to LAPW, this leads to a reduction in setup time of the nonspherical part by a factor 16.

If one performs a calculation with linearized polarization l-quantum numbers one has to choose between APW+lop and L/APW+lo basis sets. The APW+lop basis set adds polarization lo's which increases both the number of basis functions and, as the lo's contain a $b^{\alpha,lo}_{L}\dot{u}^{\alpha}_{1l}(r')$ term, reduces the advantage of the simpler basis set form in the nonspherical part of the Hamilton setup. Thus the APW+lop basis is potentially expensive in, e.g., closed-packed structures containing heavy elements. Treating the polarization l with LAPW means that hardly any speed-up due to the simpler form of the basis functions is gained. The most elegant solution seems to be to treat all physically important l as APW with added lo's, the first polarization l as an LAPW and the rest as APW. The difference between the pure APW+lo and the APW basis sets with linearized polarization orbitals are only significant for highly accurate calculations. A pure APW+lo basis set should therefore be adequate at normal PW cutoffs. It should still be kept in mind that the differences in computational time between the different APW+lo, APW+lop and L/APW+lo basis sets are small compared to the considerable reduction in computational time compared to a pure LAPW basis set.

IV. CONCLUSION

The total-energy convergence of Cu_2O has been analyzed and it has been found that when the energy dependence of all l components are linearized, as they are automatically in LAPW, the APW+lo basis set converges to the same total energy as LAPW. Thereby it has been demonstrated that the linearization used in APW+lo is as efficient as in LAPW.

Through an analysis of a minimal basis set calculation on bcc Fe it was shown that the requirement in LAPW of continuous derivatives at the MT border deformes the radial functions away from their optimal form. This is especially true for basis functions that have a strong energy dependence inside the sphere.

Generally we have found that considerable computational savings can be achieved by employing an APW+lo basis set. It has been shown that results obtained with the APW+lo converges faster and often more systematically towards the final value. Thereby accurate calculations can be performed at a much lower cost than with the LAPW basis set. There is no doubt that the APW+lo method promises very large savings for larger structures and allows reliable treatment of systems that were previously unaccessible to LAPW due to computational limitations.

ACKNOWLEDGMENTS

G.K.H.M. gratefully acknowledges a Post Doc funded by the Training and Mobility Network on ''Electronic Structure Calculations of Materials Properties and Processes for Industry and Basic Sciences'' (Contract FMRX-CT98-1078) and financed through the Forschungs Zentrum Jülich, Germany. E.S. and L.N. acknowledge the financial support from the Swedish Natural Science Research Council and support from the Ψ_k network during the stay in Vienna. P.B. and K.S. were supported in part by the Austrian Science Foundation (SFB Project F1108). We thank David J. Singh and Stefan Blügel for interesting discussions.

APPENDIX A: HAMILTON MATRIX ELEMENTS

As APW's are not constrained to have continuous derivatives at the MT boundaries and according to Green's theorem a surface integral over the sphere of discontinuity must be added[16] to the kinetic energy contribution of the Hamilton matrix,

$$T_{\mathbf{K},\mathbf{K}'} = \int_{V_I} (\nabla \phi_{\mathbf{K}})^* \cdot \nabla \phi_{\mathbf{K}'} d\mathbf{r} + \sum_{\alpha} \left(\int_{V^{\alpha}_{MT}} \phi^{*}_{\mathbf{K}} (-\nabla^2) \phi_{\mathbf{K}'} d\mathbf{r} + \oint_{S^{\alpha}_{MT}} \phi^{*}_{\mathbf{K}} \nabla \phi_{\mathbf{K}'} d\mathbf{S} \right), \tag{A1}$$

where S^{α}_{MT} is the boundary surface, V_I is the volume of the interstitial region, V^{α}_{MT} is the volume of the MT sphere around atom α. The surface element $d\mathbf{S}$ is directed outwards from the enclosed volume. The one electron wave functions can retain the discontinuity in slope of the basis functions at the MT surface. However, it has only little effect on observable properties and disappears as variational freedom is improved with increasing basis set size.[17]

The contribution of the extra surface term to the Hamilton matrix can be shown to be (dropping the index α)

$$\oint_{S_{MT}} \phi^{*}_{\mathbf{K}} \nabla \phi_{\mathbf{K}'} d\mathbf{S} = R^2_{MT} \sum_{L} \left[a^{\mathbf{K}}_{L} u_{1l}(R_{MT}) + b^{\mathbf{K}}_{L} \dot{u}_{1l}(R_{MT}) + c^{\mathbf{K}}_{L} u_{2l}(R_{MT}) \right]^* \left[a^{\mathbf{K}'}_{L} u'_{1l}(R_{MT}) + b^{\mathbf{K}'}_{L} \dot{u}'_{1l}(R_{MT}) + c^{\mathbf{K}'}_{L} u'_{2l}(R_{MT}) \right], \tag{A2}$$

where the prime indicates the radial derivative. Depending on whether $\phi_{\mathbf{K}}$ and $\phi_{\mathbf{K}'}$ are LAPW's, APW's, or LO some of the terms in Eq. (A2) will be zero. As LO are zero at the MT boundary, the surface terms will be zero if $\phi_{\mathbf{K}}$ is a lo or a LO. It will also be zero if $\phi_{\mathbf{K}'}$ is a LO of the form defined in Eq. (3) as the derivative is zero at the MT boundary.

APPENDIX B: FORCES WITHIN THE APW+lo METHOD

In the force expression implemented into WIEN97 the force on an atom is calculated as a sum of five contributions.[8] The Hellman-Feynmann and core contributions are purely electrostatic and are therefore unchanged between APW and LAPW basis sets. Furthermore the contribution from the nonspherical potential can still be calculated as given by Yu *et al.*[8] The differences occur only in the contributions due to the surface terms contribution to the kinetic energy in the spherical Hamiltonian inside the MT sphere $\mathbf{F}^{\alpha}_{sph}$, and the surface term $\mathbf{F}^{\alpha}_{sur}$.

Using the $-\nabla^2$ operator for the kinetic energy density within the sphere one gets (dropping the index α)

$$\begin{aligned}\mathbf{F}_{sph}=\sum_{\mathbf{k},i}\ \omega_{\mathbf{k},i}\sum_{l,m}\ \mathrm{Im}(&\mathbf{A}^i_L[2A^i_L(\epsilon_{1l}-\varepsilon_i)+B^i_L+C^i_L N_{l,12}(\epsilon_{1l}\\&+\epsilon_{2l}-2\varepsilon_i)]^*+\mathbf{B}^i_L\{2B^i_L(\epsilon_{1l}-\varepsilon_i)\dot{N}_l+A^i_L\\&+C^i_L[\dot{N}_{l,12}(\epsilon_{1l}+\epsilon_{2l}-2\varepsilon_i)+N_{l,12}]\}^*\\&+\mathbf{C}^i_L[2C^i_L(\epsilon_{2l}-\varepsilon_i)+B^i_L N_{l,12}+(A^i_L N_{l,12}+B^i_L\dot{N}^{\alpha}_{l,12})\\&\times(\epsilon_{1l}+\epsilon_{2l}-2\varepsilon_i)]^*),\end{aligned}\tag{B1}$$

where

$$N_{l,12}=\langle u_{1l}|u_{2l}\rangle,\quad \dot{N}_l=\langle\dot{u}_{1l}|\dot{u}_{1l}\rangle,\ \ \dot{N}_{l,12}=\langle\dot{u}_{1l}|u_{2l}\rangle\tag{B2}$$

and

$$A^i_L=\sum_{\mathbf{K}}\ c_{\mathbf{K},i}a^{\mathbf{K}}_L,\ \ \mathbf{A}^i_L=\sum_{\mathbf{K}}\ \mathbf{K}c_{\mathbf{K},i}a^{\mathbf{K}}_L\tag{B3}$$

and equivalently for B and C. $c_{\mathbf{K},i}$ denotes the variational coefficients of the ith eigenstate. Furthermore, a contribution from the surface term, Eq. (A1), must be added to $\mathbf{F}_{sph}$,

$$\begin{aligned}\sum_{\mathbf{k},i}\ \omega_{\mathbf{k},i}\sum_{l,m}\ \mathrm{Im}[&R^2_{MT}\{[A^i_L u_{1l}(R_{MT})+B^i_L\dot{u}_{1l}(R_{MT})\\&+C^i_L u_{2l}(R_{MT})]^*[\mathbf{A}^i_L u'_{1l}(R^{\alpha}_{MT})+\mathbf{B}^i_L\dot{u}'_{1l}(R_{MT})\\&+\mathbf{C}^i_L u'_{2l}(R_{MT})]-[\mathbf{A}^i_L u_{1l}(R_{MT})+\mathbf{B}^i_L\dot{u}_{1l}(R_{MT})\\&+\mathbf{C}^i_L u_{2l}(R_{MT})]^*[A^i_L u'_{1l}(R_{MT})+B^i_L\dot{u}'_{1l}(R_{MT})\\&+C^i_L u'_{2l}(R_{MT})]\}].\end{aligned}\tag{B4}$$

The choice of representing a movement of an atom by moving the corresponding MT sphere, as done in Ref. 8, yields a surface term in the force expression.[13] This surface term involves the kinetic energy operator, defined by the $\nabla\cdot\nabla$ operator, and is given as

$$\begin{aligned}\mathbf{F}^{\alpha}_{sur}&=\sum_{\mathbf{k},i}\ \omega_{\mathbf{k},i}\oint_{S^{\alpha}_{MT}}\psi^*_i(\hat{T}-\varepsilon_i)\psi_i|_I d\mathbf{S}\\&=\sum_{\mathbf{k},i}\ \omega_{\mathbf{k},i}\sum_{\mathbf{K},\mathbf{K}'}\ (c^*_{\mathbf{K},i}c_{\mathbf{K}',i})[(\mathbf{K}+\mathbf{k})\\&\quad\cdot(\mathbf{K}'+\mathbf{k})-\varepsilon_i]\oint_{S^{\alpha}_{MT}}\phi^*_{\mathbf{K}}\phi_{\mathbf{K}'I}d\mathbf{S}.\end{aligned}\tag{B5}$$

Where the I indicates that the integral should be evaluated using the interstitial wave functions. Originally $\mathbf{F}^{\alpha}_{sur}$ was evaluated using the MT wave functions.[8] With APW basis functions this procedure is no longer valid because the derivatives of the basis functions are no longer required to be continuous on the MT border.

However, in the interstitial region, a kinetic energy density, defined by a $\hat{T}-\varepsilon_i$ operator, can be expressed as a single sum over symmetrized Fourier coefficients, equivalently to the expression of the electron density in the interstitial region,

$$T(\mathbf{r})=\sum_{\mathbf{G}}\ T_{\mathbf{G}}e^{i\mathbf{G}\cdot\mathbf{r}},\tag{B6}$$

where $\mathbf{G}$ runs over all unique $\mathbf{K}'-\mathbf{K}$. The Fourier expansion of the charge density in the interstitial region can be evaluated by series of fast Fourier transforms (FFT's),[18] and the coefficients $T_{\mathbf{G}}$ can be evaluated by a similar procedure:

$$\begin{aligned}&(K_x+k_x)c_{\mathbf{K},i}\rightarrow^{FFT}T_{i,x}(\mathbf{r}),\ \ (K_y+k_y)c_{\mathbf{K},i}\rightarrow^{FFT}T_{i,y}(\mathbf{r}),\\&(K_z+k_z)c_{\mathbf{K},i}\rightarrow^{FFT}T_{i,z}(\mathbf{r}),\\&c_{\mathbf{K},i}\rightarrow^{FFT}\psi_i(\mathbf{r})\sum_{\mathbf{k},i}\ \omega_{\mathbf{k},i}[T^*_{i,x}(\mathbf{r})T_{i,x}(\mathbf{r})+T^*_{i,y}(\mathbf{r})T_{i,y}(\mathbf{r})\\&\quad+T^*_{i,z}(\mathbf{r})T_{i,z}(\mathbf{r})-\varepsilon_i\psi^*_i(\mathbf{r})\psi_i(\mathbf{r})]=T(\mathbf{r})\rightarrow^{FFT}T_{\mathbf{G}}.\end{aligned}\tag{B7}$$

The force can then be evaluated as a sum over the symmetrized kinetic energy coefficients,

$$\mathbf{F}^{\alpha}_{sur}=\sum_{\mathbf{G}}\ T_{\mathbf{G}}\oint_{S^{\alpha}_{MT}}e^{i\mathbf{G}\cdot\mathbf{r}}d\mathbf{S}.\tag{B8}$$

By expanding the PW's into spherical Bessel functions the surface integral can be shown to be

$$\oint_{S_{\alpha}}e^{i\mathbf{G}\cdot\mathbf{r}}d\mathbf{S}_{\alpha}=i\mathbf{G}\begin{cases}\dfrac{4\pi}{3}R^3_{MT} & \mathbf{G}=0\\[2ex]\dfrac{4\pi}{|\mathbf{G}|}R^2_{MT}j_1(|\mathbf{G}|R_{MT})e^{i\mathbf{G}\cdot\mathbf{r}_{\alpha}} & \mathbf{G}\neq 0\end{cases}.\tag{B9}$$

It should be pointed out that the use of the $\nabla\cdot\nabla$ operator

changes $\mathbf{F}_{sph}$ and $\mathbf{F}_{sur}$ also for LAPW basis sets. However, as the LAPW's are differentiable the differences cancel out. Hence the total force calculated on an atom with LAPW is exactly the same as when using the expressions in Ref. 8. The expressions for $\mathbf{F}_{sph}$, Eqs. (B1) and (B4), and $\mathbf{F}_{sur}$, Eqs. (B8) and (B9), are therefore completely general.

[1] J.C. Slater, Phys. Rev. **51**, 151 (1937).
[2] T.L. Loucks, *Augmented Plane Wave Method* (W.A. Benjamin, Inc., New York, 1967).
[3] O.K. Andersen, Phys. Rev. B **12**, 3060 (1975).
[4] D.D. Koelling and G.O. Arbman, J. Phys. F: Met. Phys. **5**, 2041 (1975).
[5] D. Singh, Phys. Rev. B **43**, 6388 (1991).
[6] E. Sjöstedt, L. Nordström, and D.J. Singh, Solid State Commun. **114**, 15 (2000).
[7] P. Blaha, K. Schwarz, and J. Luitz, *WIEN97, A Full Potential Linearized Augmented Plane Wave Package for Calculating Crystal Properties* (Tech. Universität Wien, Austria, 1999).
[8] R. Yu, D. Singh, and H. Krakauer, Phys. Rev. B **43**, 6411 (1991).
[9] P.E. Blöchl, O. Jepsen, and O.K. Andersen, Phys. Rev. B **49**, 16 223 (1994).
[10] P. Blaha, K. Schwarz, W. Faber, and J. Luitz, Hyperfine Interact. **126**, 389 (2000).
[11] P. Blaha and K. Schwarz, Hyperfine Interact **52**, 153 (1989).
[12] G.K.H. Madsen, C. Gatti, B.B. Iversen, L. Damjanovic, G.D. Stucky, and V.I. Srdanov, Phys. Rev. B **59**, 12 359 (1999); G.K.H. Madsen, B.B. Iversen, P. Blaha, and K. Schwarz, Phys. Rev. B (to be published).
[13] E. Sjöstedt, Licentiate thesis, Uppsala University, Sweden, 1999.
[14] D. Singh, Phys. Rev. B **40**, 5428 (1989).
[15] E. Wimmer, H. Krakauer, M. Weinert, and A.J. Freeman, Phys. Rev. B **24**, 864 (1981).
[16] P.M. Marcus, Int. J. Quantum Chem. **1S**, 567 (1967).
[17] B.N. Harmon, D.D. Koelling, and A.J. Freeman, J. Phys. C **6**, 2294 (1973).
[18] D.J. Singh, *Planewaves, Pseudopotential and the LAPW Method* (Kluwer Academic, Boston, Dordrecht, London, 1994).